Annals of Biomedical Engineering, Vol. 38, No. 2, February 2010 *(© 2010)* pp. 259–268
DOI: 10.1007/s10439-009-9845-4

Use of a Novel Robotic Interface to Study Finger Motor Control

E. G. Cruz[1,2] and D. G. Kamper[2,3]

[1]Department of Biomedical Engineering, Northwestern University, Evanston, IL 60208, USA; [2]Sensory Motor Performance Program, Rehabilitation Institute of Chicago, Chicago, IL 60611, USA; and [3]Department of Biomedical Engineering, Illinois Institute of Technology, 314 Wishnick Hall, Chicago, IL 60616, USA

(Received 22 May 2009; accepted 14 November 2009; published online 25 November 2009)

Abstract—Stroke is the leading cause of permanent adult disability in the U.S., frequently resulting in chronic motor impairments. Rehabilitation of the upper limb, particularly the hand, is especially important as arm and hand deficits post-stroke limit the performance of activities of daily living and, subsequently, functional independence. Hand rehabilitation is challenging due to the complexity of motor control of the hand. New instrumentation is needed to facilitate examination of the hand. Thus, a novel actuated exoskeleton for the index finger, the FingerBot, was developed to permit the study of finger kinetics and kinematics under a variety of conditions. Two such novel environments, one applying a spring-like extension torque proportional to angular displacement at each finger joint and another applying a constant extension torque at each joint, were compared in 10 stroke survivors with the FingerBot. Subjects attempted to reach targets located throughout the finger workspace. The constant extension torque assistance resulted in a greater workspace area ($p < 0.02$) and a larger active range of motion for the metacarpophalangeal joint ($p < 0.01$) than the spring-like assistance. Additionally, accuracy in terms of reaching the target was greater with the constant extension assistance as compared to no assistance. The FingerBot can be a valuable tool in assessing various hand rehabilitation paradigms following stroke.

Keywords—Stroke, Hand rehabilitation, Motor control.

INTRODUCTION

Motor control of the hand is a complicated task. For the index finger alone, tendons from seven different muscles insert on the three phalanges. Each of these tendons crosses more than one joint, thereby influencing joint torque production at multiple joints. Even relatively simple movements of the finger require coordinated activity from a number of muscles.[8] Thus, the study of motor control of the hand can be complex, especially following neuromuscular injury such as stroke. Of the roughly 425,000 individuals who survive a stroke in a given year,[21] 50% will have some form of chronic impairment,[25] typically involving weakness of the hand.[21,27] The limited finger extension associated with hemiparesis greatly reduces the function of the hand in activities of daily living.[28] While a number of factors have been examined for contributions to impairment following stroke,[4,18,20] the mechanisms of this impairment have not been fully elucidated. Additionally, the effects of different rehabilitation strategies, such as error augmentation,[19] guided-force training,[10] and passive assistance,[22] are not well understood.

Instrumentation permitting quantified assessment of rehabilitation paradigms and of finger motor control under a variety of imposed conditions would thus be beneficial. Indeed, use of robots in the study of the upper extremity has greatly contributed to knowledge of motor control of the arm, both in stroke surviors[19] and in individuals without neurological impairment.[26] For simplicity, the apparatus could be designed to examine a single finger, with the assumption that results obtained for this digit would be representative of those expected in the other fingers due to the extensive neurophysiological coupling that exists across the digits.[14] The index finger is the most likely choice for the representative digit due to: its functional importance as the primary finger involved in tip and lateral grasps; its greater voluntary individuation of movement in comparison with its other fingers[14]; and its accessibility. This system would necessarily require the ability to provide independent control or perturbations of each of the three finger joints.

A number of devices have been developed which can actuate the digits of the hand. These devices include both commercial products, such as the CyberGrasp™ (VRLOGIC GmbH, Dieburg, Germany) and Amadeo® (Tyromotion GmbH, Graz, Germany), and research systems, such as the Rutgers Hand Master II,[9] HWARD,[24] a haptic interface,[16] and a cable-driven exoskeleton.[29] As these devices were developed with other criteria in mind, however, they do not provide

Address correspondence to D. G. Kamper, Department of Biomedical Engineering, Illinois Institute of Technology, 314 Wishnick Hall, Chicago, IL 60616, USA. Electronic mail: kamper@iit.edu

the independent control of each joint of the index finger with sufficient power to serve as a general purpose platform for examining motor control.

Thus, the goals of this study were to develop a novel motorized exoskeleton, the FingerBot, to independently actuate each of the three joints of the index finger and to assess the feasibility of use of this exoskeleton in the stroke population. The FingerBot was employed to examine the impact of two different types of assistance on motor control of the hand post-stroke. The use of devices providing passive assistance of movement, such as through springs, to facilitate training during rehabilitation therapy is growing. For example, four commercial devices for stroke rehabilitation, the WREX (JAECO Orthopedic, Hot Springs, AR, USA), the Armeo (Hocoma AG, Zurich, Switzerland), the Armeo Boom (Hocoma AG, Zurich, Switzerland), and the SaeboFlex (Saebo, Inc., Charlotte, NC, USA) all utilize spring-like mechanisms. This passive actuation has advantages in terms of weight, responsiveness, and safety. For given implementations, however, it may actually impede movement in certain directions. A large assistance extension torque provided about a joint through springs, for instance, may hinder joint flexion, especially in stroke survivors, whose paretic limb is often weak.[3,7] Thus, certain types of assistance may be preferable to maximize motion for training. For this study, two such modes of assistance which could be implemented in passive devices, a constant extension bias and a spring-like restoring bias, were compared in an effort to better guide the development of future devices and training paradigms.

MATERIALS AND METHODS

FingerBot Design

The actuated exoskeleton, the FingerBot, consists of a series of linkages which parallel the corresponding finger segments. It is attached to the distal, middle, and proximal segments of the finger. Three servomotors, one aligned with each anatomical joint of the index finger, are located at the joints between the linkages. Thus, actuation of a given servomotor can produce flexion/extension of the corresponding metacarpophalangeal (MCP), proximal interphalangeal (PIP) or distal interphalangeal (DIP) joint (Fig. 1). Each joint can thereby be controlled independently. The complete FingerBot system is designed to completely support its own weight, as well as the weight of the index finger. The distal support system design (Fig. 1) affords little resistance to movements in the sagittal plane as a result of the double bearing design applied at each of its joints. Yet, it constrains finger movement to the sagittal plane of the finger.

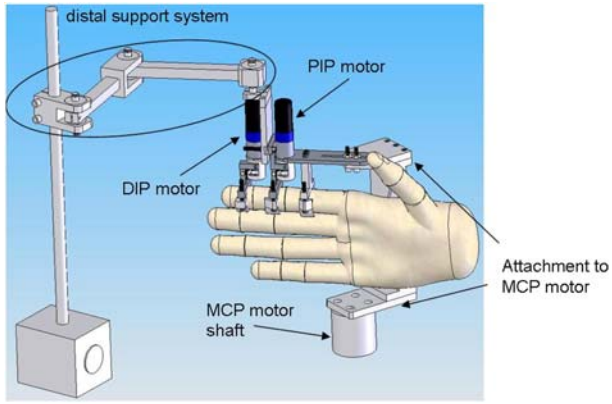

FIGURE 1. SolidWorks (SolidWorks Corp., Concord, MA) drawing of the complete FingerBot exoskeleton design. The motor driving the MCP joints resides below the hand, while the motors for the PIP and DIP joints reside above the index finger and move with it.

By using the actuated exoskeleton design rather than a device coupled to the fingertip, potential problems with singularities, leading to instability[23] and propagation of errors down the kinematic chain when computing inverse kinematics or kinetics, can be mitigated. Importantly, the potentially uncomfortable joint constraint forces inherently produced by devices coupled to the fingertip can be avoided. For example, to independently control the three-joint torques, two orthogonal forces and a moment would need to be applied at the fingertip. These forces produce corresponding joint reaction forces in the DIP, PIP, and MCP joints. For example, to generate 2.0 N m of torque at the MCP joint and no torque at the DIP and PIP joints for a finger posture of (MCP, PIP, DIP) flexion angles = (30°, 30°, 0°), a resultant force vector of 80 N would have to be applied along the long axis of the distal segment (see Appendix). For 0.5 N m of torque at the PIP joint and no torque at the MCP and DIP joints at this same posture, an external resultant force vector of 52 N, along with an external torque, would be required. Errors in the direction of this force vector (directional errors can easily result from slip between the fingertip and the actuation device) can lead to significant errors in the joint torques (see Fig. A.1 in Appendix).

The Fingerbot is coupled to the finger through the use of custom-fabricated components. Each interface has a set of two bolts that thread into a slightly concave aluminum upper piece. The bottom of the interface is made from acetal plastic (Delrin®) and features a contoured U-shape that fits comfortably against the medial surface of each finger segment (Fig. 2). The U-shaped interface pieces mate with corresponding

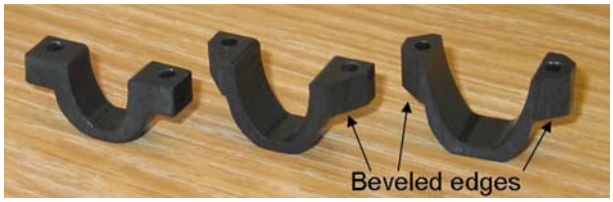

FIGURE 2. U-pieces for interfacing with finger.

TABLE 1. Population anthropometrics.

	Segment lengths (cm)	
	Proximal	Middle
Maximum	5.46	3.05
Minimum	3.91	2.34
Average (SD)	4.72 (0.41)	2.69 (0.24)

$n = 31$ (12 stroke survivors).

concave pieces attached to the exoskeleton, thereby providing maximal contact with the finger and distribution of pressure.

One difficulty inherent to the exoskeleton design is sizing the device to fingers of varying lengths. To estimate the possible segment lengths that would need to be accommodated by the FingerBot, a convenience sample of 31 individuals (19 males and 12 females) was measured (see Table 1 for summary).

The results of this study were used to generate an estimate of the true characteristics of the population from which subjects will be drawn. A large ($n = 500$) normally distributed random sample was generated using the parameters of this test sample. Thus, the FingerBot was designed to accommodate an estimated 99% of the population, with proximal segment lengths ranging from 3.3 to 6.35 cm and middle segment lengths ranging from 2.29 to 3.56 cm. Adjustments for differently sized finger segments are located at the slot connecting the C-piece with the rest of the FingerBot and the connection between the shaft of the PIP motor and the DIP motor (see Fig. 3). The device can accommodate the index finger of either hand. The other fingers are allowed to assume a relaxed posture beneath the index finger. Wrist position and orientation are maintained by placing the wrist in a fiberglass cast and securing that cast to the same table as the FingerBot.

The U-pieces do impose subject-specific physical limitations on joint range of motion (ROM). The comfortable ROM at each joint within the FingerBot device was determined for a set of 17 subjects. The average (ROM) for these subjects was found to be 58.8° at the MCP joint, 68.9° at the PIP joint, and 57.6° at the DIP joint. These values represent 53.4, 68.9, and 76.8% of the physiological range of motion at MCP, PIP, and DIP, respectively,[17] and should be sufficient for most intervention evaluations. Mechanical stops are present at all joints to prevent excessive flexion or extension. Additional proximity sensors are set at the ends of the desired range of motion for the MCP joints. The sensors immediately kill the more powerful MCP actuator when tripped.

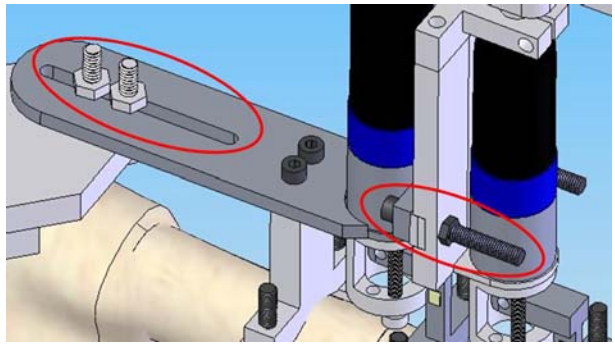

FIGURE 3. FingerBot adjustment features with each point of adjustment outlined as drawn in SolidWorks.

A direct-drive servomotor (JR16M4CH-1, PMI Motion Technologies, KollMorgen Co.) serves as the actuator for the MCP joint. It is controlled with a pulse-width modulated servo amplifier (AXA-180-10-30, PMI Motion Technologies) and contains both an optical encoder (HA625-2500, DynaTECH, Elm Grove Village, IL) and tachometer (PMI Motion Technologies). A torque sensor (TRT-200, Transducer Techniques, Temecula, CA) is coupled between the motor shaft and the hand interface to record the joint torques generated. The direct-drive motor can provide sufficient torque and speed to match the performance of the MCP joint.

For the two motors which move with the finger, coreless DC micro motors (MicroMo Model #1724, Clearwater, FL) were chosen to actuate the PIP and DIP joints. These motors are small in size (17 mm in diameter), lightweight (26.9 g), and relatively powerful (up to 4 Watts). Each motor is coupled to a planetary gearhead (MicroMo Model #16/7) with a 66:1 reduction ratio. Motor position is sensed using magnetic encoders (MicroMo Model #IE2-512). Despite the high gear ratio, these motors are still backdrivable due to the small motor intertia.

The FingerBot is controlled by a computer running a real time operating system on an x86 platform (QNX Software Systems; Ottawa, ON). Control signals are sent through a D/A board (KPCI-3130, Keithley Instruments; Cleveland, OH) to the motor amplifiers. Angle and/or torque feedback control can be implemented at each joint. Velocity and torque signals are sampled through an A/D board (DAS-1800HR,

Keithley Instruments), while the motor positions are sampled using a PC encoder board (5312, PC Encoder, Technology 80 Inc., Minneapolis, MN). The current software arrangement allows for the FingerBot to be operated using three torque control options: spring-like, constant torque, and passive. Each of these modes utilizes a proportional-integrative-derivative feedback (torque or position) control algorithm for the MCP motor. The distal motors utilize an open-loop algorithm when controlling torque and a closed-loop feedback algorithm when controlling position.

Experimental Design

Subjects

First, five individuals without any known neurological or orthopedic impairment were recruited for a small pilot study to ensure proper device performance.

Then, 10 stroke survivors with chronic hemiparesis were recruited for this study to compare the impact of two different types of finger assistance on finger motor control. Potential subjects were evaluated by a research occupational therapist to ensure appropriateness for the study. Inclusionary criteria included: hand impairment resulting from a single stroke experienced at least 9 months prior to enrollment in the study, passive range of motion of the affected hand equal to or greater than the motion allowed by the FingerBot, and visually discernible active finger flexion and extension.

All subjects signed a consent form approved by the Institutional Review Board of Northwestern University that outlined the protocol, risks, and subject rights. Participant information, including age, years post-stroke, and passive range of motion within the FingerBot, is shown in Table 2. All tests were performed on the index finger of the impaired hand (6 left hand, 4 right hand) of stroke survivors or the dominant hand (all right) of control subjects.

Experimental Protocol

Subjects performed a set of point-to-point movements with the fingertip in the sagittal plane while the finger resided within the FingerBot. A fiberglass cast was secured around the subject's forearm and wrist to fix the wrist angle in neutral. The cast was clamped to the tabletop to prevent translation of the hand with respect to the FingerBot.[13] The subject's finger was then placed inside the FingerBot and the joints were aligned with the axis of each motor.

Subjects performed movements while the FingerBot provided one of three assistance modes: spring-like extension, constant extension, and passive. The spring-like mode is intended to simulate the presence of a torsional spring at each joint by providing an extension torque proportional to the angular displacement away from the neutral position:

$$\tau = k(\theta - \theta_r) \quad (1)$$

where k is the spring constant and θ_r is the neutral resting angle (0° flexion at MCP, PIP, and DIP). Four different spring constants were employed for each motor and thus each joint. These constants spanned the range of spring constants provided with the SaeboFlex^{TM} system (Saebo, Inc., Charlotte, NC), a commercial orthosis which uses springs to move the digits toward extension. The spring constant chosen for a given subject was the minimum of the set which would keep the joint at 35° of flexion or less when at rest.

For constant extension assistance, a constant extension torque was used at each joint. This extension torque was set equal to the torque required to keep the joint in the neutral position of 0° of flexion or extension ($\tau = \tau_{neutral}$). For the MCP motor, the average extension torque across all stroke subjects was 0.46 N m. For the PIP joint the average for all stroke survivors was 0.66 N m, and for the DIP joint the average was 0.03 N m.

While in the passive mode, the Fingerbot allowed for free movement of the finger. Servo control for zero torque was employed for the MCP motor to account for its impedance while the two more distal motors were disabled.

Subject fingertip position was represented as a cursor on a monitor in front of the subject. The experimental task consisted of moving the fingertip cursor to the same position as a green target presented on the monitor at a random location within the workspace of the finger. Once the subject reached and held the target for 250 ms, an audio signal was generated and the target changed from green to magenta to cue success. If 12 s elapsed before the subject was able to reach the target a different sound was heard and the target

TABLE 2. Subject information.

Group	Age	Years post-stroke	MCP ROM	PIP ROM	DIP ROM
Stroke ($n = 10$)	67.6 ± 8.9	8.8 ± 4.7	58.6 ± 7.8	68.9 ± 4.6	57.2 ± 5.9

Mean ± standard deviation.
ROM given in degrees.

changed to red. Three-seconds of rest followed each target trial and the subject was able to take short breaks after every ten targets if desired. The starting position for each trial was unconstrained. This process was repeated for the same 64 targets under each setting (passive, spring-like, constant extension), for a total of 192 experimental trials. Target locations were chosen such that the required joint postures spanned the passive joint ranges of motion for each subject. Prior to the experimental trials the subject performed practice trials to familiarize him/herself with the apparatus and screen feedback system.

Data Analysis

The primary analysis examined the kinematic workspace of each individual under the three conditions. The fingertip positions, obtained throughout the trials in a given assistance mode, were calculated according to the following forward kinematic equations:

$$\begin{aligned} x &= l^*_{DP}\sin(\theta_{MCP}+\theta_{PIP}+\theta_{DIP}) + l^*_{MP}\sin(\theta_{MCP}+\theta_{PIP}) \\ &\quad + l^*_{PP}\sin(\theta_{MCP}) \\ y &= l^*_{DP}\cos(\theta_{MCP}+\theta_{PIP}+\theta_{DIP}) + l^*_{MP}\cos(\theta_{MCP}+\theta_{PIP}) \\ &\quad + l^*_{PP}\cos(\theta_{MCP}) \end{aligned} \quad (2)$$

where l_{DP}, l_{MP}, and l_{PP} are the measured distal, middle, and proximal phalanx segment lengths, and θ_{MCP}, θ_{PIP}, and θ_{DIP} are the measured joint angles. The outputs from this equation are the x and y location in a coordinate system whose origin is the center of the MCP joint (Fig. 4). All of the fingertip positions attained for a given condition formed a set describing a workspace cluster.

The area of this cluster of points was then calculated using convex hulls[1] in a custom MATLAB routine.[11] The area of the theoretical workspace was similarly calculated for each subject using his/her passive range of motion within the FingerBot. The area attained under each condition was then expressed as a percentage of this theoretical maximum area.

The theoretical workspace was divided into two sub-regions to examine any changes in the location of the fingertip under the modes of assistance. The midpoint between the maximum and minimum y-values of the theoretical workspace was used to split the workspace in two; the percent area attained for each of these regions was computed.

Additionally, the range of motion at each joint was calculated for each condition to examine any joint-specific kinematic changes. Joint range was computed from the maximum and minimum joint angles for each joint for a given assistance level. The final outcome measure examined was the average minimum distance

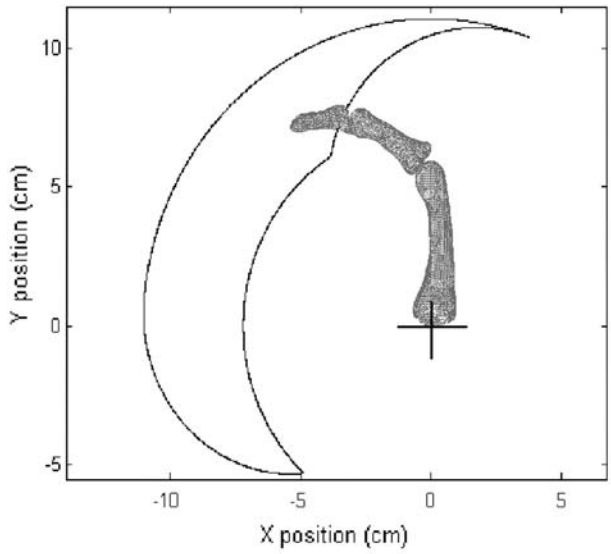

FIGURE 4. Anatomical orientation of coordinate frame used to examine kinematic data. Three segments and joints are shown, with the location of the MCP joint marked (+). The theoretical workspace within the FingerBot is outlined.

from the intended target. This was computed to provide some insight as to the level of performance under each condition. A lower average minimum distance would indicate the subject was on average closer to the target.

The five outcomes were then examined in a doubly MANOVA (SPSS Inc, Chicago, IL) with a within-subject factor of mode of assistance. As mode of assistance showed significance, each outcome was further analyzed with a univariate split-plot ANOVA. *Post hoc* pairwise comparisons (Bonferroni adjustment) were performed to determine statistically significant different levels of a factor. The level of significance applied for all results was $\alpha = 0.05$.

RESULTS

Ten stroke survivors participated in this study to assess index finger kinematics. Subjects performed a target matching task while the FingerBot system provided one of three different assistance modes to each joint of their finger: constant extension, spring-like, and passive. The same set of tasks was performed with the FingerBot in each of the three settings.

The results of the doubly MANOVA demonstrated that the independent factor of assistance had a significant (Wilk's lambda $p < 0.001$) impact on the outcome measures collected. Further univariate ANOVAs were then performed for each dependent variable.

The results for the kinematic workspace area showed a significant effect of assistance condition

($p = 0.001$). The pairwise comparisons of the estimated marginal means revealed a significant ($p = 0.011$) difference, with the constant extension mode yielding an area greater than that of the spring-like mode by 19.3% ± 15.6% of the total theoretical workspace (Fig. 5). The difference between the constant extension condition and the passive condition (13.8% ± 15.2% of the total theoretical workspace) was also large, although marginally insignificant ($p = 0.056$). The difference between the spring-like and passive conditions (−5.6% ± 10.4%) was insignificant ($p = 0.329$).

Most of the increase in workspace occurred in the upper region, thereby indicating a greater ability to extend the finger (see Fig. 6 for an example). Pairwise comparisons confirmed a significant ($p = 0.011$) difference in the upper sub-region between constant extension and the spring-like conditions ($p = 0.033$) and between the constant extension condition and the passive condition ($p = 0.011$). Further, the results for the lower sub-region demonstrated a significant ($p = 0.011$) difference between the constant extension and spring-like conditions, as well as between the spring-like condition and the passive condition ($p = 0.003$). In summary, the constant extension assistance significantly increased the workspace in the upper sub-region compared to the passive condition (Δ23% ± 19% of theoretical workspace), while the spring-like assistance significantly reduced the workspace in the lower sub-region relative to the passive condition (Δ16% ± 11% of theoretical workspace).

The joint range of motion data showed statistically significant effects ($p < 0.05$) of condition for MCP, but not for DIP or PIP (Fig. 6). The pairwise comparisons indicated an increase in MCP joint range under the constant extension condition (Δ7.9°, $p = 0.01$) when compared with the passive condition (Fig. 7). Further, the spring-like mode significantly ($p = 0.006$) decreased (−Δ7.3°) the range of motion at the MCP joint from the passive condition. Thus, a

FIGURE 5. Kinematic workspace results across assistance conditions for stroke survivors. Error bars denote 95% confidence intervals.

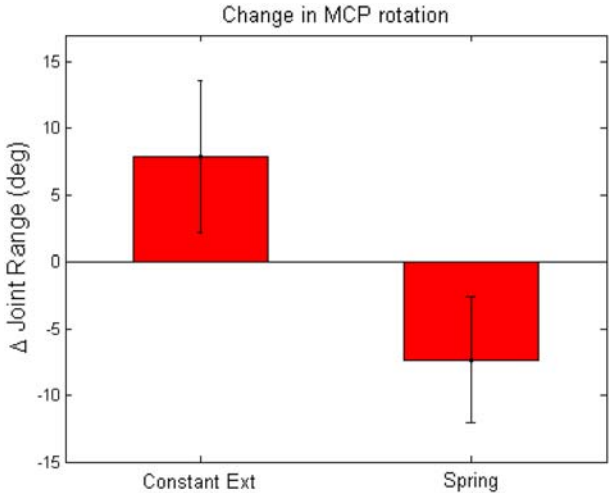

FIGURE 7. Difference in active range of MCP rotation across stroke survivors for the constant extension and spring conditions in comparison with the passive condition. Error bars denote 95% confidence intervals.

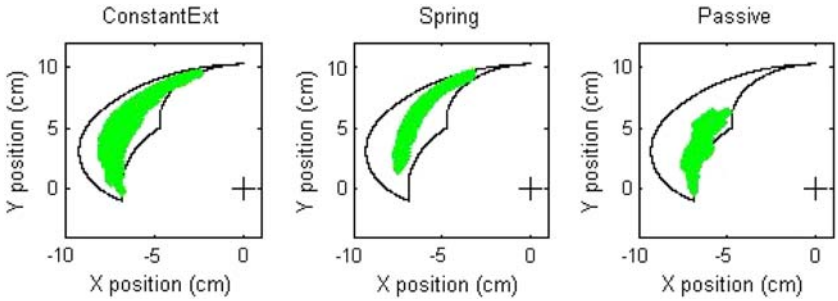

FIGURE 6. Complete set of workspace data for a single stroke subject under each assistance condition. Shaded area indicates region traversed by index fingertip. For this particular subject, the percent theoretical areas calculated were 34.7, 15.4, and 17.4% for the constant extension, spring, and passive settings, respectively.

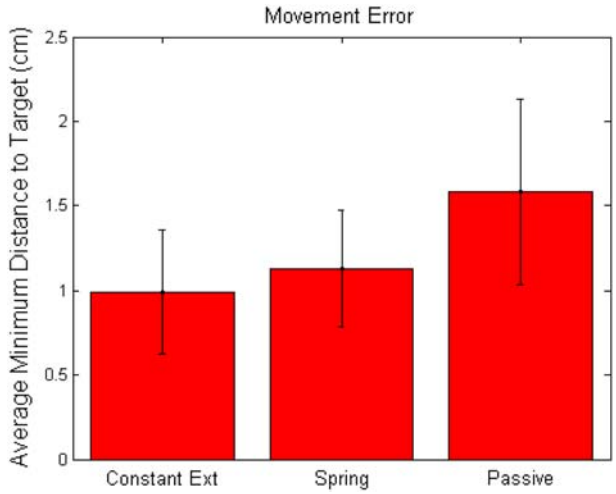

FIGURE 8. Average minimum distance from target for stroke survivors under the different assistance conditions. Error bars denote 95% confidence intervals.

significant difference of 15.2° between the constant extension and spring settings was recorded ($p < 0.001$).

The average minimum distance from the target revealed a dependence upon assistance condition for stroke survivors (Fig. 8). The constant extension mode was significantly better than the passive mode in terms of proximity to target ($p = 0.044$), with an average difference of 5.9 ± 6.2 mm. The difference between the spring-like and passive conditions (4.6 ± 8.4 mm) was not found to be significant ($p = 0.361$).

DISCUSSION

The FingerBot was successfully used to examine motor control in the target population of stroke survivors. Specifically, we found that different types of finger assistance had significantly different effects on finger motor control.

Without any assistance, stroke subjects covered 30% of the theoretical workspace; with constant extension torque assistance this rose to 44%. Workspace area under the constant extension condition was 57% larger than that produced under the spring-like condition. This difference is likely due to the inability of users to generate sufficient flexion torque to overcome the spring-like bias, which increases with finger flexion angle. Furthermore, the MCP range of motion also revealed a significant decrease between the constant extension and spring-like conditions. This also indicates that despite the residual flexion strength seen in stroke survivors, weakness persists, in accordance with published findings.[5,12] Subjectively, participants reported that targets requiring flexion of the MCP and PIP joints were more difficult or impossible to reach in the spring setting due to the higher torque levels acting against the intended motion.

Examination of the sub-regions of the workspace further supported the functional benefits seen under the constant extension mode. The constant extension mode increased the area in the upper sub-region more than the spring-like mode with respect to the passive mode. This upper region has been shown to be important for the completion of functional tasks.[11] While the spring-like condition was able to moderately increase this upper region workspace, it also produced a significant decrease in the lower sub-region. The original hypothesis that a constant extension mode can increase the workspace by providing assistance while permitting flexion movements was thus supported. It must be noted that the attainment of a posture does not guarantee any degree of function at that posture. Further testing would need to be performed to assess the functional capacity throughout the workspace under different assistance conditions.

This study also compared the average error (minimum distance of fingertip position to the target) between conditions. A shorter distance implies that the user was able to more accurately reach the intended target. The significant difference between the constant extension and passive conditions indicates that the constant extension condition does on average provide some improvement in accuracy. The functional importance of the difference observed (0.59 cm), however, remains to be adequately explored.

To investigate a potential cause of the observed differences in workspace, the range of motion at each joint was examined under each condition. These data revealed a significant difference in MCP range of motion between the assistance conditions. It is therefore likely that the differences in workspace area between conditions are a result of the MCP range of motion. Forward kinematics was used to predict the effect a change in MCP joint range would have on the total workspace. This analysis revealed that a 7° change in joint range (the difference noted between the constant extension and passive conditions) would result in a workspace change of 9–12%, depending on the segment lengths. This may also indicate that stroke survivors are relatively weaker in MCP flexion than PIP flexion, as the PIP range of motion was not significantly different between conditions. This joint-dependent weakness may be related to the higher passive stiffness of the MCP joint.[15]

Stroke survivors had particular difficulty in simultaneously controlling their digits to move in opposite directions. For example, postures requiring flexion of the MCP joint while keeping PIP and DIP near neutral were extremely difficult for subjects to attain. Likewise,

postures requiring little MCP flexion but significant flexion of the PIP and DIP joint presented a similar level of difficulty. It appears that once a single joint is flexed, all of the joints are biased toward flexion, creating difficultly in extension tasks. This supports the previously described observations of a generalized flexor bias seen in stroke survivors.[2]

Future studies using similar protocols would benefit from addressing the limitations of this study. The duration of the study, approximately 2 h, may have led to a lack of attention and/or motivation for stroke survivors toward the end of the testing session. While this did not appreciably impact the results of this study, the effects should be avoided. Another important validation that needs to be performed is the comparison of the kinematic results obtained from the FingerBot assistance conditions and the current clinical applications which they mimic (e.g., an actual spring-actuate glove). Another limitation of this study is the incomplete workspace exploration resulting from the experimental protocol. The workspace area attained by the five control subjects represented on average 80% of the theoretical workspace. This limitation could be addressed by increasing the workspace from which the random targets are selected beyond that of the theoretical workspace. The current protocol used the maximum comfortable range of motion within the FingerBot for each subject to generate the theoretical workspace from which the target locations were chosen. By randomly selecting points within this workspace the outer edges of this workspace will not necessarily be included in the target task. This was originally avoided to limit the level of frustration for stroke survivors, leading to the incomplete workspace analysis of control subjects. Increasing the target area would ensure that subjects attempted to reach all points within the theoretical workspace. This limitation did not impact the results of this study as significant differences in workspace area were still noted.

CONCLUSION

The results presented here demonstrate the utility of the FingerBot device in the analysis of finger biomechanics and rehabilitation. In particular, this study suggests that a constant extension torque bias produces a larger kinematic workspace than a spring-like torque bias at the finger joints for stroke survivors. Introduction of the constant-torque assistance led to an increase of 14% of the *total theoretical workspace* over what could be attained with no assistance. This equates to almost 50% of the area that could be reached without assistance. The feasibility of increasing not just extension, but the active workspace and range of motion is encouraging. A splint, in contrast, can increases extension, but at the cost of drastically reducing active range of motion.

Importantly, control of finger movement improved significantly as well, as evidenced by the decrease in the error to the target. Thus, the constant extension torque bias would allow greater and more precise exploration of the finger workspace for rehabilitative practice. These findings are directly applicable to the design of orthotic gloves for use in rehabilitation training after stroke.

Future studies will examine the effectiveness of new rehabilitation strategies, such as error augmentation[19] and a compliant, adaptive assistance.[30] While these modes have been tested with the arm, motor control of the hand may differ.[6] The flexibility and control offered by the FingerBot makes it a useful platform for evaluating these techniques before attempting to implement them for the whole hand.

APPENDIX

The Jacobian matrix (J) relating the three joint torques $\left(\boldsymbol{\tau} = \begin{bmatrix} \boldsymbol{\tau}_{\mathbf{MCP}} \\ \boldsymbol{\tau}_{\mathbf{PIP}} \\ \boldsymbol{\tau}_{\mathbf{DIP}} \end{bmatrix}\right)$ to the forces and moment $\left(\mathbf{f} = \begin{bmatrix} \mathbf{F_x} \\ \mathbf{F_y} \\ \boldsymbol{\tau}_{\mathbf{z}} \end{bmatrix}\right)$ at the fingertip is given by Eq. A.1:

$$J = \begin{bmatrix} -l_P \sin(\vartheta_P) - l_M \sin(\vartheta_P + \vartheta_M) & & \\ \quad - l_D \sin(\theta_P + \theta_M + \theta_D) & - l_M \sin(\vartheta_P + \vartheta_M) - l_D \sin(\theta_P + \theta_M + \theta_D) & - l_D \sin(\theta_P + \theta_M + \theta_D) \\ l_P \cos(\vartheta_P) + l_M \cos(\vartheta_P + \vartheta_M) & & \\ \quad + l_D \cos(\theta_P + \theta_M + \theta_D) & l_M \cos(\vartheta_P + \vartheta_M) + l_D \cos(\theta_P + \theta_M + \theta_D) & l_D \cos(\theta_P + \theta_M + \theta_D) \\ 1 & 1 & 1 \end{bmatrix} \tag{A.1}$$

where, l_P is the length of proximal finger segment, l_M is the length of middle finger segment, l_D is the length of distal finger segment, θ_P is the MCP flexion/extension angle, θ_M is the PIP flexion/extension angle, and θ_D is the DIP flexion/extension angle.

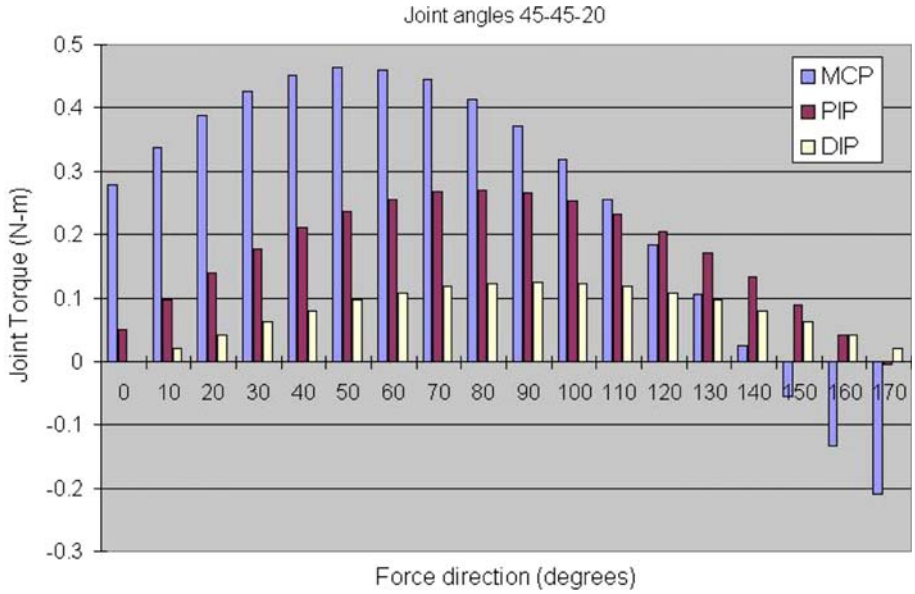

FIGURE A.1. The torques resulting at each of the three finger joints from an input force of 5 N directed at the fingertip. Finger posture, in terms of (MCP, PIP, DIP) flexion joint angles, is (45°, 45°, 20°). Force direction refers to degrees between the input force vector and the vector described by the distal phalanx (0° denotes a force directed along the long axis of the distal phalanx toward the DIP joint). Positive torque signifies an extension torque.

The joint torques are related to the fingertip forces/moment by:

$$\tau = J^{\mathrm{T}} f \qquad \text{(A.2)}$$

Changes in the angle with respect to the fingertip of an applied force affects the joint torques generated. The changes are not uniform across the joints. For example, altering the force direction from 80° with respect to the long axis of the distal segment to 100° has minimal effect on the PIP and DIP torques, but has a significant effect on the MCP torque (Fig. A.1).

ACKNOWLEDGMENTS

This work was supported by a grant from the Coleman Foundation. We wish to thank Dr. Edward Colgate and Dr. Eric Perreault for their insightful recommendations regarding the design of the FingerBot and of the experiment and Mr. Dan Qiu for his examination of the sensitivity of the Jacobian matrix.

REFERENCES

[1]Barber, C. B., D. P. Dobkin, and H. T. Huhdanpaa. The Quickhull algorithm for convex hulls. *ACM Trans. Math. Software* 22:469–483, 1996.
[2]Beer, R. F., J. P. Dewald, M. L. Dawson, and W. Z. Rymer. Target-dependent differences between free and constrained arm movements in chronic hemiparesis. *Exp. Brain Res*. 156:458–470, 2004.
[3]Canning, C. G., L. Ada, R. Adams, and N. J. O'Dwyer. Loss of strength contributes more to physical disability after stroke than loss of dexterity. *Clin. Rehabil*. 18:300–308, 2004.
[4]Canning, C. G., L. Ada, and N. J. O'Dwyer. Abnormal muscle activation characteristics associated with loss of dexterity after stroke. *J. Neurol. Sci*. 176:45–56, 2000.
[5]Chae, J., G. Yang, B. K. Park, and I. Labatia. Muscle weakness and cocontraction in upper limb hemiparesis: relationship to motor impairment and physical disability. *Neurorehabil. Neural Repair* 16:241–248, 2002.
[6]Cruz, E. G., and D. G. Kamper. Kinematics of point-to-point finger movements. *Exp. Brain Res*. 174:29–34, 2006.
[7]Cruz, E. G., H. C. Waldinger, and D. G. Kamper. Kinetic and kinematic workspaces of the index finger following stroke. *Brain* 128:1112–1121, 2005.
[8]Darling, W. G., and K. J. Cole. Muscle activation patterns and kinetics of human index finger movements. *J. Neurophysiol*. 63:1098–1108, 1990.
[9]Jack, D., R. Boian, A. S. Merians, M. Tremaine, G. C. Burdea, S. V. Adamovich, M. Recce, and H. Poizner. Virtual reality-enhanced stroke rehabilitation. *IEEE Trans. Neural Syst. Rehabil. Eng*. 9:308–318, 2001.
[10]Kahn, L. E., P. S. Lum, W. Z. Rymer, and D. J. Reinkensmeyer. Robot-assisted movement training for the stroke-impaired arm: does it matter what the robot does? *J. Rehabil. Res. Dev*. 43:619–630, 2006.
[11]Kamper, D. G., E. G. Cruz, and M. P. Siegel. Stereotypical fingertip trajectories during grasp. *J. Neurophysiol*. 90:3702–3710, 2003.
[12]Kamper, D. G., H. C. Fischer, E. G. Cruz, and W. Z. Rymer. Weakness is the primary contributor to finger impairment in chronic stroke. *Arch. Phys. Med. Rehabil*. 87:1262–1269, 2006.

[13]Kamper, D. G., and W. Z. Rymer. Quantitative features of the stretch response of extrinsic finger muscles in hemiparetic stroke. *Muscle Nerve* 23:954–961, 2000.
[14]Lang, C. E., and M. H. Schieber. Human finger independence: limitations due to passive mechanical coupling versus active neuromuscular control. *J. Neurophysiol.* 92: 2802–2810, 2004.
[15]Li, Z. M., G. Davis, N. P. Gustafson, and R. J. Goitz. A robot-assisted study of intrinsic muscle regulation on proximal interphalangeal joint stiffness by varying metacarpophalangeal joint position. *J. Orthop. Res.* 24:407–415, 2006.
[16]Mali, U., N. Goljar, and M. Munih. Application of haptic interface for finger exercise. *IEEE Trans. Neural Syst. Rehabil. Eng.* 14:352–360, 2006.
[17]Mallon, W. J., H. R. Brown, and J. A. Nunley. Digital ranges of motion: normal values in young adults. *J. Hand. Surg. [Am.]* 16:882–887, 1991.
[18]Patten, C., J. Lexell, and H. E. Brown. Weakness and strength training in persons with poststroke hemiplegia: rationale, method, and efficacy. *J. Rehabil. Res. Dev.* 41: 293–312, 2004.
[19]Patton, J. L., M. E. Stoykov, M. Kovic, and F. A. Mussa-Ivaldi. Evaluation of robotic training forces that either enhance or reduce error in chronic hemiparetic stroke survivors. *Exp. Brain Res.* 168:368–383, 2006.
[20]Powers, R. K., J. Marder-Meyer, and W. Z. Rymer. Quantitative relations between hypertonia and stretch reflex threshold in spastic hemiparesis. *Ann. Neurol.* 23: 115–124, 1988.
[21]Rosamond, W., K. Flegal, G. Friday, K. Furie, A. Go, K. Greenlund, N. Haase, M. Ho, V. Howard, B. Kissela, S. Kittner, D. Lloyd-Jones, M. McDermott, J. Meigs, C. Moy, G. Nichol, C. J. O'Donnell, V. Roger, J. Rumsfeld, P. Sorlie, J. Steinberger, T. Thom, S. Wasserthiel-Smoller, and Y. Hong. Heart disease and stroke statistics—2007 update: a report from the American Heart Association Statistics Committee and Stroke Statistics Subcommittee. *Circulation* 115:e69–e171, 2007.
[22]Sanchez, R. J., J. Liu, S. Rao, P. Shah, R. Smith, T. Rahman, S. C. Cramer, J. E. Bobrow, and D. J. Reinkensmeyer. Automating arm movement training following severe stroke: functional exercises with quantitative feedback in a gravity-reduced environment. *IEEE Trans. Neural Syst. Rehabil. Eng.* 14:378–389, 2006.
[23]Spong, M. W., S. Hutchinson, and M. Vidyasagar. Robot Modeling and Control. London: John Wiley & Sons, Inc, 2006.
[24]Takahashi, C. D., L. Der-Yeghiaian, V. Le, R. R. Motiwala, and S. C. Cramer. Robot-based hand motor therapy after stroke. *Brain* 131:425–437, 2008.
[25]Thom, T., N. Haase, W. Rosamond, V. J. Howard, J. Rumsfeld, T. Manolio, Z. J. Zheng, K. Flegal, C. O'Donnell, S. Kittner, D. Lloyd-Jones, D. C. Goff, Jr., Y. Hong, R. Adams, G. Friday, K. Furie, P. Gorelick, B. Kissela, J. Marler, J. Meigs, V. Roger, S. Sidney, P. Sorlie, J. Steinberger, S. Wasserthiel-Smoller, M. Wilson, and P. Wolf. Heart disease and stroke statistics—2006 update: a report from the American Heart Association Statistics Committee and Stroke Statistics Subcommittee. *Circulation* 113:e85–e151, 2006.
[26]Thoroughman, K. A., and R. Shadmehr. Learning of action through adaptive combination of motor primitives. *Nature* 407:742–747, 2000.
[27]Trombly, C. Occupational Therapy for Physical Dysfunction. Baltimore: Williams and Wilkins, 1989.
[28]Wade, D. The Epidemiologically Based Needs Assessment Reviews, Vol. I. Oxford: Radcliffe Medical Press, pp. 111–255, 1994.
[29]Wege, A., and A. Zimmerman. Electromyography sensor based control for a hand exoskeleton. In: IEEE International Conference on Robotics and Biomimetics, Sanya, China, 2007, pp. 1470–1475.
[30]Wolbrecht, E. T., V. Chan, D. J. Reinkensmeyer, and J. E. Bobrow. Optimizing compliant, model-based robotic assistance to promote neurorehabilitation. *IEEE Trans. Neural Syst. Rehabil. Eng.* 16:286–297, 2008.